Nanoscale Advances

Accepted Manuscript

This article can be cited before page numbers have been issued, to do this please use: T. Khandaker, A. B. M. Ibrahim, W. S. Al-Rashed, K. I. Anojaidi, W. A. Al-Suwaylih, M. A. Al-Suwaylih, M. A. Habib and M. S. Hossain, *Nanoscale Adv.*, 2025, DOI: 10.1039/D5NA00996K.

ROYAL SOCIETY OF CHEMISTRY

rsc.li/nanoscale-advances

View Article Online
DOI: 10.1039/D5NA00996K

Sustainable Wastewater Treatment Using Novel Zeolite-Polymer (ZePol) Composite Materials

Tasmina Khandaker,[a] Ahmed B.M. Ibrahim,[b] Wael S. Al-Rashed,[c] Khalid I. Anojaidi,[d] Waleed A. Al-Suwaylih,[d] Mohammed A. Al-Suwaylih,[d] Mohamed A. Habib,[b] Muhammad Sarwar Hossain[e]*

[a]Department of Chemistry, Khulna Khan Bahadur Ahsanullah University, Khulna-9100, Bangladesh.
[b]Department of Chemistry, College of Science, Imam Mohammad Ibn Saud Islamic University (IMSIU), Riyadh 11623, Saudi Arabia.
[c]Department of Civil Engineering, Faculty of Engineering, University of Tabuk, P.O. Box 741, Tabuk 71491, Saudi Arabia.
[d]King Abdulaziz City for Science and Technology (KACST), Riyadh 11442, Saudi Arabia.
[e]Chemistry Discipline, Khulna University, Khulna-9208, Bangladesh
*Correspondence: sarwar@chem.ku.ac.bd

Abstract

Emergence of effective, durable treatment technology is of paramount importance due to the rising threat of toxic heavy metal pollution of water resources to human health as well as the environment. In order to improve multi-functional adsorption, we present the synthesis and performance of ZePol-4, a novel zeolite-polymer composite made from ETS-4 zeolite, chitosan, polyvinyl alcohol (PVA), and L-cysteine. The crystallinity, porosity, and functional group integrity of the composite were validated by structural and morphological characterizations (XRD, SEM, and EDS). Excellent uptake capacities for important heavy metals were shown by batch adsorption experiments, with equilibrium adsorption capacities of 243.5 mg/g (Pb^{2+}), 170.1 mg/g (Hg^{2+}), 113.5 mg/g (Cu^{2+}), 80.3 mg/g (Cd^{2+}), and 45.3 mg/g (As^{3+}). In accordance with this, ZePol-4 obtained high removal efficiencies in 60 minutes of 98% for Pb^{2+}, 93% for Cd^{2+}, 88% for Hg^{2+}, 75% for As^{3+}, and 70% for Cu^{2+}. The composite required less extensive chemical adjustment because it worked well over a broad pH range, with optimal removal taking place close to neutral pH. The accuracy of the removal data was guaranteed by dual quantification using UV-Vis and ICP-MS. Strong binding interactions and quick kinetics were made possible by the complementary contributions of amino, hydroxyl, and thiol groups through surface complexation and ion exchange. With its quick adsorption, high selectivity, and operational compatibility with actual environmental conditions, ZePol-4 shows great promise as a scalable, environmentally friendly, and highly effective material for tertiary wastewater treatment.

View Article Online
DOI: 10.1039/D5NA00996K

Keywords: Zeolite-Polymer Composite (Zepol), Heavy Metal Adsorption, Wastewater treatment, Environmental remediation.

1. Introduction

Human activities, particularly the release of untreated wastewater into the natural environment, have significantly contributed to the world's ongoing environmental problem. Urban areas produce around 75-80% of water usage as wastewater and are therefore a major contributor to the problem. In the same vein, industrial processes produce a large amount of polluted water, which is compounded by the application of new chemical substances. Water bodies are highly contaminated because of the speedy growth of industrialization and lack of proper wastewater treatment processes, threatening public health and environmental balance [1, 2]. Heavy metals, dyes, organic materials, grease, and oil are among the wastewater contaminants that seriously endanger aquatic ecosystems and public health. Because of their toxicity, persistence, and capacity for bioaccumulation, toxic heavy metals such as lead, mercury, cadmium, chromium, and copper are especially hazardous. By contaminating seafood, these metals endanger marine biodiversity, upset food chains, and seriously endanger human health. The problem is made worse by the breakdown of biodegradable materials in wastewater, which lowers dissolved oxygen levels, which are necessary for aquatic life [3, 4]. Heavy metals can enter the environment from a variety of sources, such as untreated household wastewater, agricultural runoff from metal-laden fertilizers and pesticides, and industrial discharges [5]. Following their release, they persist in soils and water, disrupting the natural balance and entering the food chain, leading to biomagnification and prolonged exposure. Strict monitoring, effective waste treatment technologies, and sustainable industrial and agricultural practices are necessary to address these concerns and safeguard ecosystems and public health [6, 7].

Addressing the issue of heavy metal contamination in wastewater requires the use of effective and durable treatment methods. Traditional methods such as coagulation, sedimentation, and filtration have demonstrated difficulties in the treatment of complex wastewater compositions and the removal of heavy metal traces [8]. Furthermore, the economics and ecology are negatively impacted by these methods since they usually result in excessive sludge production or require expensive chemical reagents. Advanced approaches such as chemical precipitation, membrane separation, ion exchange, electrodialysis, and adsorption have been studied; due to its cost, high removal

View Article Online
DOI: 10.1039/D5NA00996K

efficiency, and convenience of use, adsorption has emerged as a very promising solution [9]. The practical problems with conventional adsorbents, however, have spurred the creation of new materials. Many people are interested in zeolite-based materials because of its unique properties, which include their high surface area, powerful ion-exchange capabilities, and exceptional chemical stability. Zeolites are particularly successful at selectively eliminating heavy metals from wastewater because to these properties, making them an economical and sustainable alternative to traditional treatment methods. It is possible to optimize removal efficiency while minimizing adverse impacts on the economy and environment by focusing on these innovative materials, paving the way for safer and cleaner water management systems [10]. Zeolite polymer synthesis is an approach that shows promise for revolutionizing wastewater treatment and providing a practical option for enhanced heavy metal removal. Zeolite polymers combine the advantages of zeolites and polymers to create products with enhanced stability, greater selectivity, and tunable properties. These substances can be designed to specifically target heavy metal ions, even at low concentrations, ensuring efficient removal [11].

The natural biopolymer chitosan, which is made by deacetylating chitin, found in crab shells, has several advantages due to its non-toxic, biodegradable, and biocompatible properties. The compound, which is composed of β-(1-4)-linked N-acetyl-D-glucosamine and D-glucosamine units, has significant applications in water purification and environmental repair. Because of its high porosity and water solubility, chitosan is a valuable material for metal ion adsorption. This allows it to effectively attach to heavy metals such as cadmium, lead, and mercury. It is used increasingly often in industrial and environmental cleanup processes due to its ability to stick to negatively charged surfaces and oil spills, creating a more environmentally friendly environment[12]. The water-soluble, biodegradable polymer PVA is known for its self-cross-linking ability and biocompatibility due to its hydroxyl groups; however, it is bioinert and hydrolyzes rapidly. Numerous goods, including detergents, dyes, and chemicals for water treatment, include PVA, which is safe for human exposure based on sub-chronic toxicity and genotoxicity studies. For water purification, PVA produces polymer composites with natural zeolites that have superior adsorption and ion-exchange properties. The aldehyde-modified zeolite is expected to react with chitosan's amino groups through aldehyde-amine condensation, forming imine (Schiff base) bonds that enhance interfacial adhesion and strengthen the composite structure. Alongside these covalent linkages, additional stability is provided by hydrogen bonding among PVA's hydroxyl groups,

View Article Online
DOI: 10.1039/D5NA00996K

chitosan's functional groups, and the zeolite's silanol groups. Aldehyde–chitosan Schiff bases also exhibit rapid hydrolysis under mildly acidic conditions (pH 4-6), releasing over 39% of aldehydes within 10 hours. This aldehyde release improves their antibacterial performance, showing greater effectiveness at pH 5 than at neutral pH [13]. The aldehyde-functionalized zeolite, chitosan, PVA, and L-cysteine most likely interacted covalently and non-covalently to produce the composite. Covalent anchoring points between the inorganic and polymeric phases can be created by the aldehyde groups on the modified zeolite reacting with the primary amines of chitosan to create imine (Schiff base) connections. In order to create a physically crosslinked network that improves flexibility and film formation, chitosan and PVA mainly interact through substantial hydrogen bonding between their hydroxyl and amine groups. There are several ways to integrate L-cysteine: Its carboxyl and thiol groups can engage in hydrogen bonding with PVA and chitosan; its amine group can also create imine bonds with any remaining aldehyde groups on the zeolite surface; and electrostatic interactions can take place. There are several ways to incorporate L-cysteine: (i) its amine group can also form imine bonds with any remaining aldehyde groups on the zeolite surface; (ii) its carboxyl and thiol groups can participate in hydrogen bonding with PVA and chitosan; (iii) under slightly acidic conditions, protonated chitosan ($–NH_3^+$) and deprotonated cysteine ($-COO^-$) can interact electrostatically; and (iv) thiol groups can oxidize to form disulfide linkages, which provide additional crosslinking. Zeolite provides covalent anchoring, chitosan provides structural connectivity, PVA gives mechanical flexibility, and L-cysteine introduces functional thiol chemistry to create a hybrid organic–inorganic network. To effectively remove heavy metals and phenols from water, these composites make use of the hydrophilic and porous characteristics of zeolites. These materials are most successful when used using methods such as melt-mixing compounding, and factors such as zeolite loading and solution pH significantly boost their efficacy. They are helpful in applications that need high performance, such as flame retardants, automotive parts, and construction materials, particularly when reinforced with hydrophilic fillers[14]. A variety of functional groups, such as thiol (-SH), carboxyl (-COOH), and amino ($-NH_2$) groups, are present in amino acids (AAs), which are vital biomolecules. Of these, L-cysteine (L-Cys) has attracted more attention lately because of its straightforward molecular structure, ease of accessibility, and eco-friendliness [15]. Through grafting, it has been demonstrated that the addition of L-cysteine improves material performance. Today, this sulfur compound is incorporated into reasonably priced, cost-efficient materials. According to the hard and soft acid-base (HSAB)

View Article Online
DOI: 10.1039/D5NA00996K

principle, the thiol (-SH) group of L-cysteine is very drawn to heavy metal ions, while the carboxyl (-COOH) and thiol (-SH) groups can interact with heavy metals [16]. L-cysteine is mostly absorbed into the polymeric network through hydrogen bonding via –SH, $–NH_2$, and –COOH groups as well as electrostatic interactions with the protonated amino groups of chitosan. Additionally, the thiol group of L-cysteine may interact with the surface functional groups of the modified zeolite to help immobilize it within the composite. Even though covalent attachment to the polymer backbone is less feasible at the synthesis conditions used, the multi-point noncovalent contacts allow L-cysteine to be progressively incorporated into the matrix [17].

One of the best techniques for purifying water systems of contaminants is adsorption. Commonly used materials include polymers, biomass, activated carbon, and zeolite; zeolite-polymer composites have become especially effective adsorbents because of their high ability to remove heavy metals at low concentrations. The use of hybrid zeolite-biopolymer adsorbents has grown in popularity in recent years. For example, zeolite-chitosan beads were created to remove Cd(II) and Pb(II), and magnetically modified zeolite–polymer composites were used to remove several heavy metals at once [18, 19]. To improve Hg(II) uptake, another study showed how to add thiol-functionalized polymers to natural zeolite frameworks [20]. Few studies have examined the particular combination of ETS-4, a titanosilicate zeolite, with a dual biopolymer binder (chitosan and PVA) and a targeted thiol-bearing amino acid ligand (L-cysteine), despite the fact that these works clearly demonstrate the benefits of combining zeolite frameworks with biopolymer or polymeric modifiers. In the present work, the structural robustness and high cation-exchange potential of ETS-4 are combined with the film-forming and binding versatility of a chitosan-PVA network. The composite is further functionalized with L-cysteine to introduce -SH and $-NH_2$ active moieties that can chelate strongly with both soft and hard heavy-metal ions. As a result, this synthesis is novel not only because it uses a zeolite and polymer binder, but also because it introduces multifunctional ligands in a customized way into a single composite platform, improving selectivity, kinetics, and uptake capacities in comparison to previous zeolite-polymer systems. Using cutting-edge methods to decipher intermolecular interactions and the underlying adsorption mechanisms, this study explores the application of zeolite-chitosan-cellulose polymer composites for heavy metal adsorption. The study emphasizes a sustainable method of eliminating heavy metals from wastewater, including copper, lead, arsenic, mercury, and cadmium, by concentrating on synthesis techniques. In order to lessen the serious risks that non-biodegradable metal

View Article Online
DOI: 10.1039/D5NA00996K

contaminants pose to the environment and human health; the results highlight the urgent need for tertiary treatment in industrial effluent management. This work introduces a new process for synthesis and emphasizes the scalability, regenerability, and environmental safety compliance of zeolite-polymer composites. Although zeolite polymers possess remarkable potential, there is limited research and development in this field to date. The characterization techniques, performance evaluation, and synthesis procedures of zeolite polymers for metal removal should be studied further. We also need to look at the scalability, cost-effectiveness, and ruggedness of these materials in order to present their viability in large-scale wastewater treatment plants.

2. Methodology

2.1 Materials

For functionalizing Zeolite ETS-4 with aldehyde (-CHO) groups, 2-aminopropyl triethoxysilane (APTES), glutaraldehyde, and Zeolite ETS-4 were utilized. Polyvinyl alcohol (PVA) and L-cysteine were additionally utilized, while TCI provided the chitosan. The zeolite polymer composites were made by reacting ETS-4 (-CHO), chitosan PVA, and L-cysteine at room temperature for one hour at a speed of 25,000 rpm. PVA, or polyvinyl alcohol, was supplied by Sigma-Aldrich. Two distinct composite compositions of zeolite polymers were created, respectively, with component ratios of 4:1:2:1:0.02 and 4:1:1:0.03. Every substance and reagent were utilized just as it was delivered; no further purification was necessary.

2.2 Methods

2.2.1 Synthesis of Zeolite Polymers composite: Synthesize ZePol composite using a modified method based on reported literature [21-26]. The synthesis procedure illustrated in Figure 1 consists of the following steps:

2.2.2 Preparation of Zeolite (-CHO)

Initially, Zeolite (ETS-4) is synthesized following the standard hydrothermal synthesis method as described in the literature [21]. Briefly, titanium and silica precursors are mixed in an alkaline medium, and the resulting gel is subjected to hydrothermal treatment at an optimized temperature and duration to yield crystalline ETS-4 zeolite. After synthesis, the zeolite is filtered, washed thoroughly with deionized water, and dried at 100°C overnight.

View Article Online
DOI: 10.1039/D5NA00996K

Functionalization of ETS-4 is carried out by the reaction of 3-(aminopropyl) triethoxysilane (APTES) with the prepared Zeolite with ethyl acetate being the solvent. Zeolite (ETS-4) is suspended in ethyl acetate under ambient stirring conditions in a reactor vessel. APTES is added incrementally to the reaction mixture and allowed to react for approximately 1 h under ambient conditions. Glutaraldehyde (4.485 g) is subsequently added to the reaction mixture to allow for aldehyde functionalization (-CHO). The reaction mixture is agitated to ensure even distribution and adsorption of the aldehyde functional groups onto the zeolite surface. The functionalized zeolite is then separated by filtration, washed with ethanol to remove unreacted reagents, and dried under vacuum at 60°C for 12 h.

2.2.3 Synthesis of ZePol Composite

ZePol composite is prepared from ETS-4 (-CHO), chitosan (CS), polyvinyl alcohol (PVA), and L-cysteine. The conditions of synthesis like temperature, pH, and reactant ratios are optimized for enhancing the performance of the final composite material. For the preparation, take 10 g of ETS-4 (-CHO), 3.85 g of chitosan, 1.25 g of PVA, and 0.15 g of L-cysteine are mixed in a reaction kettle. The components are mixed with high shear mixing at 250 r.p.m. for 1 h to ensure uniform dispersion and active interaction between the components. The resulting blend is subsequently mild-heated (40-50°C) to enhance polymeric crosslinking and structural integration of the components. The pH of the reaction medium is tuned and controlled throughout the process in order to achieve the best chemical interactions.

The ZePol composite is collected after reaction, washed with deionized water to remove any unreacted residues, and vacuum-dried at 70°C for 24 h. The vacuum-dried composite is milled into fine powder for additional characterization and application studies.

2.2.4 Preparation of ZePol Thin Film

To fabricate a thin ZePol composite film, the dried ZePol powder is dissolved in an appropriate solvent, such as acetic acid, to form a homogeneous solution. The dispersion is stirred with constant agitation for 2 h to achieve homogeneity. The solution is then spin-coated onto a glass or polymer substrate. The coated substrate can be allowed to dry at room temperature for initial solvent evaporation, followed by controlled drying at 50-60°C to volatilize remaining solvent and

View Article Online
DOI: 10.1039/D5NA00996K

enhance film adhesion. The resulting thin film is also in the process of post-curing at 80°C for 2 h to further increase mechanical strength and structural integrity. The thin coating remained cohesive and stable throughout the agitation process during the batch testing. Even after constant shaking, the film did not show signs of peeling or disintegration. Long-term exposure to the aqueous environment caused some surface softening, but this did not affect the material's overall mechanical integrity or its capacity to act as an adsorbent. The film's stability was aided by its uniform thickness and elasticity, which made it resistant to mechanical stress during agitation. ZePol thin film prepared is now ready for characterization and follow-up applications.

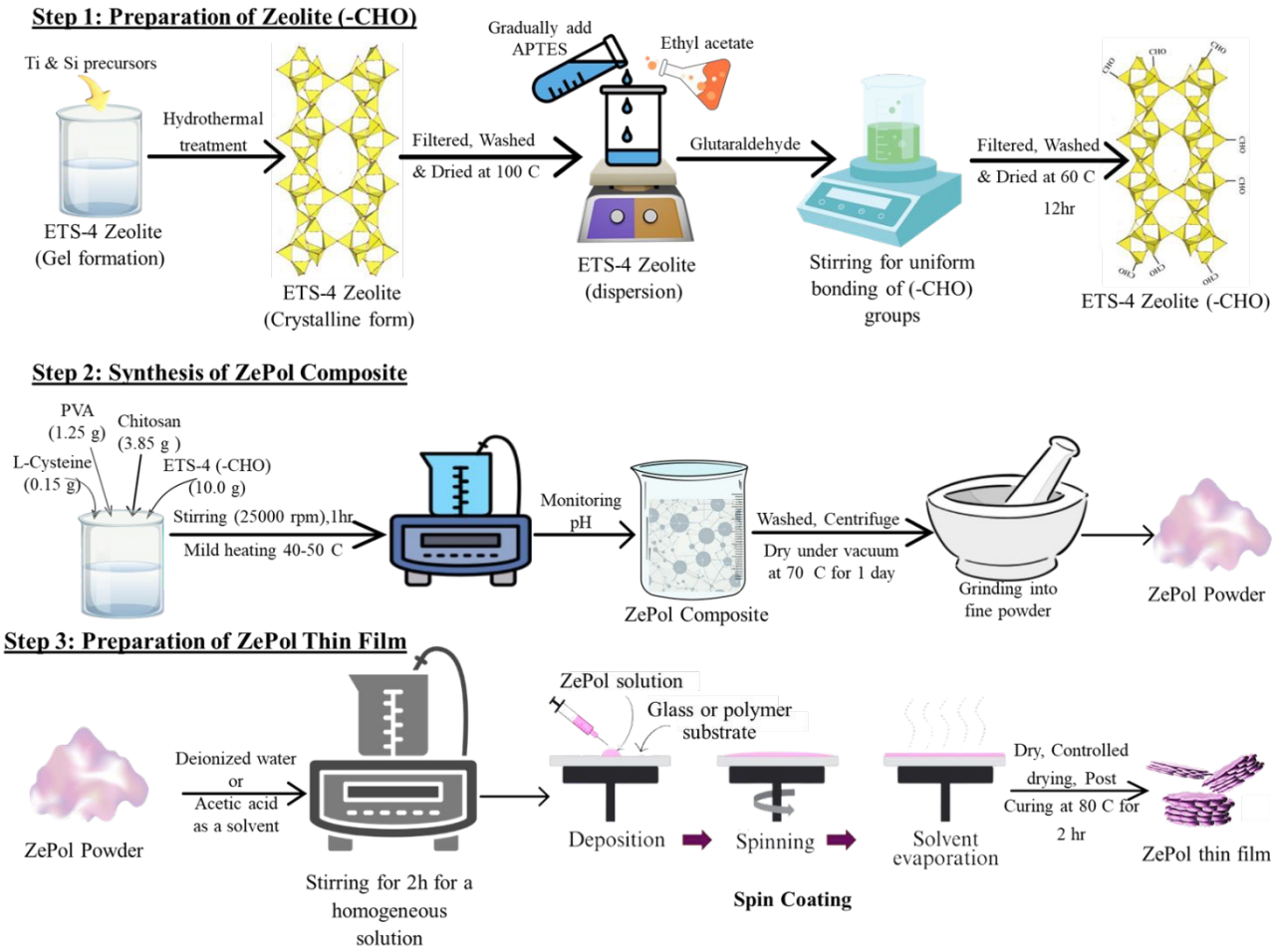

Figure 1. Schematic illustration of the Zepol synthesis process: zeolite preparation, surface modification, dispersion in a polymer matrix, spin coating, and solvent evaporation to obtain the Zepol thin film.

View Article Online
DOI: 10.1039/D5NA00996K

3. Characterization of samples

The morphological and structural characteristics of Zepol-4 composites were thoroughly investigated using a combination of advanced analytical techniques. The crystal structure was investigated by X-ray powder diffractometry (XRD) through Rigaku diffractometer with Cu Kα radiation (λ = 1.54056 Å). Scans were taken between the 2θ range of 10° to 80° in high scanning speed of 0.005° (2θ) per min to offer high-resolution diffraction patterns. The surface morphology was examined by scanning electron microscopy (SEM, Hitachi S-4300), where the structural features and texture of the surface of the film were able to be seen in great detail. For cross-sectional analysis, the thin film samples were cryogenically fractured in liquid nitrogen to preserve their microstructure and subsequently gold coated in a Magnetron Sputter Coater for 90 sec to enhance conductivity for imaging reasons. Elemental composition and distribution were investigated through energy-dispersive X-ray spectroscopy (EDS, Oxford Instruments), with particular focus on the determination of silicon-to-aluminum (Si/Al) ratio within the zeolite component. FT-IR spectra were obtained on a Thermo Scientific (Nicolet IS-50) spectrometer with the spectral range between 500 and 4000 cm^{-1} with a resolution of 4 cm^{-1} and 8 scans per scan for high signal-to-noise ratio. A MTCA detector and a potassium bromide (KBr) beam splitter were employed during the FT-IR measurements. Furthermore, UV–visible spectroscopy (Model 2550, Shimadzu, Japan) was used to assess optical properties, while inductively coupled plasma mass spectrometry (ICP-MS) enabled precise quantification of heavy metal ion concentrations in the samples.

3.1 Sorption experiments

Sorption experiments were systematically carried out using a batch adsorption approach to evaluate the performance of thin film adsorbents for heavy metal removal from synthetic wastewater. In each experiment, 50 mL of synthetic wastewater containing varying concentrations of target heavy metals was transferred into a 250 mL Erlenmeyer flask. After that, 100 mg of the prepared thin film adsorbent was added to the solution. The mixtures were agitated at 150 rpm on a 30 °C temperature-controlled shaker to enable proper contact between the adsorbate and adsorbent. Unless otherwise specified, the following experimental conditions were established as follows: particle size of Zepol < 100 µm, adsorbent-to-contaminant (A/C) mass ratio of 1:1 (g/g), initial heavy metal concentration of 100 mg/L, and constant solution pH of 5. All the samples were

View Article Online
DOI: 10.1039/D5NA00996K

filtered under vacuum upon achievement of equilibrium. The resulting supernatants were acidified and refrigerated at temperatures lower than 4 °C prior to determination of remaining metal by Inductively Coupled Plasma Mass Spectrometry (ICP-MS). Batch test was repeated three times to ensure reliability of data, and average values were employed. Efficiency of removal of heavy metals was expressed as a function of two parameters, i.e., percentage removal and adsorption capacity at equilibrium. These were determined using the following equations:

Removal rate (%) = $((C_0 - C_e)/C_0) \times 100$ ……………………………(1), and

Adsorption capacity (q_e, mg/g) = $((C_0 – C_e) \times V)/m$ …………………(2)

Where C_o and C_e are initial and equilibrium heavy metal concentration (mg/L), respectively, V is the solution volume (L), and m is the adsorbent mass (g). These experiments provided useful data on the thin film's efficiency to adsorb under controlled conditions, confirming their potential use in wastewater treatment.

4. Result and discussions

4.1 X-ray powder diffraction analysis

The X-ray diffraction (XRD) patterns provide valuable information about the structural evolution of ETS-4 upon its conversion to ZePol-4 at different reaction times (Figure-2). The native ETS-4 (lower pattern) exhibits intense and sharp diffraction peaks, indicating a highly crystalline microporous nature. Upon undergoing hydrothermal treatment to yield ZePol-4, distinct structural changes are observed. ZePol-4 sample aged for 1 h (middle pattern) retains all the characteristic peaks of ETS-4, albeit weakened in intensity and a mild broadening that reflects partial preservation of the crystalline structure. This is a reflection that a reaction time of 1 hour is sufficient to cause structural modifications without disrupting the integrity of the parent framework. On the other hand, for the longer reaction time of 3 h, ZePol-4 sample (upper pattern) shows significantly weaker peak intensities, broader reflections, and enhanced baseline noise, all of which indicate extreme loss in crystallinity.

The general structural disorder of the 3 h sample might be due to overgrowth, framework degradation by too much, or amorphous phase formation upon prolonged hydrothermal treatment. All such changes are likely to deteriorate the material's properties, such as surface area, pore

View Article Online
DOI: 10.1039/D5NA00996K

uniformity, and accessibility to adsorption sites. Therefore, the sample of ZePol-4 (1 h) has a more improved crystalline structure, maintaining the essential properties of ETS-4 and incorporating sufficient structural modifications that are expected to enhance its efficiency for uses in adsorption. The expanded and attenuated XRD peaks show that ETS-4 is still crystalline, but the polymer matrix partially blocks off its signals. Rather than a loss of crystallinity, this masking is caused by polymer encapsulation and the decreased appearance of scattered crystalline domains. This influences adsorption structurally by balancing the contributions of zeolite and polymer. The more amorphous polymer phase makes functional groups (-SH, -NH_2, -OH) more accessible, but the polymer coating restricts access to particular zeolite ion-exchange sites. As a result, adsorption results from a synergistic mechanism where polymer-driven complexation greatly reinforces ion-exchange while it is still active. The controlled level of crystallinity in the 1 h sample suggests that there is an optimum compromise between framework reactivity and stability, making it a more promising candidate compared to the over-transformed 3 h sample. The results underscore the critical role of the reaction time in controlling the structural properties of zeolite-based materials with direct relevance to their potential applications in environmental remediation and separation processes [27].

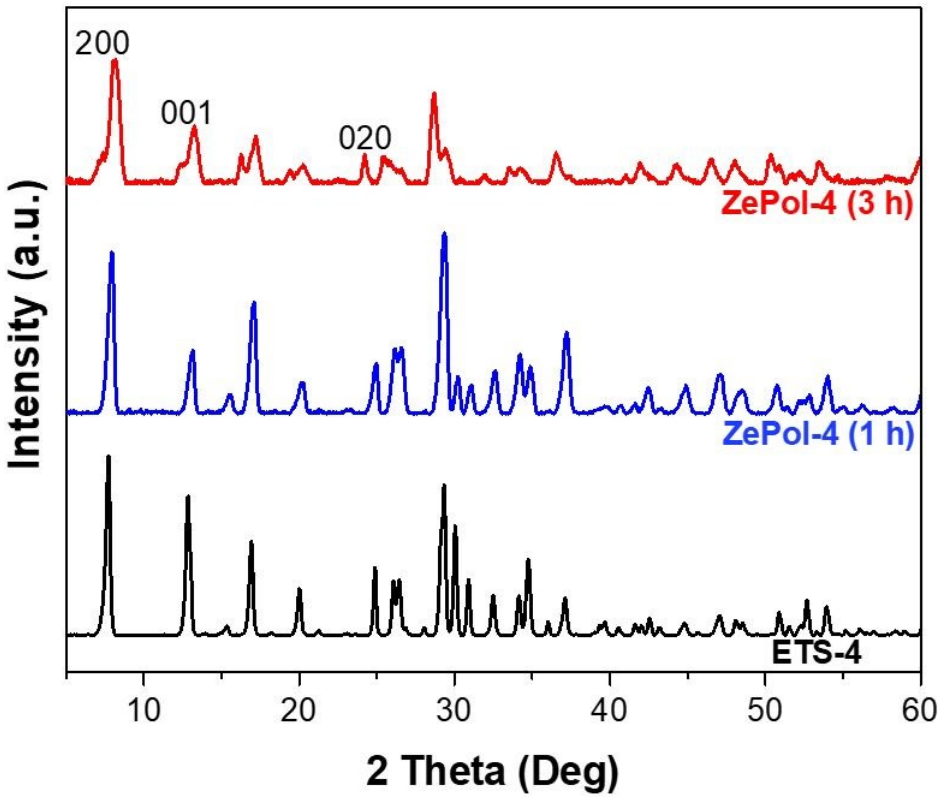

View Article Online
DOI: 10.1039/D5NA00996K

Figure 2: XRD patterns of ETS-4 and ZePol-4 synthesized at different times (1 h and 3 h), indicating phase transformation and changes in crystallinity with synthesis time.

4.2 Analysis of electron microscopy data

SEM images in figure 3 provide a close comparison of the surface morphology of ZePol-4 samples synthesized under different stirring speeds and reaction times: (i) 100–150 rpm for 24 h, (ii) 250 rpm for 1 h, and (iii) 250 rpm for 3 h. At low magnification (top row) and high magnification (bottom row), there are clear differences in surface texture and particle organization. The 100–150 rpm ZePol-4-prepared sample for 24 h (left panels) possesses a relatively dense and compact surface with large, aggregated sheets and minimal visible porosity. The morphology is very irregular, likely due to the low stirring rate, which may have been too low to disperse the reactants effectively and achieve homogeneous nucleation and crystal growth.

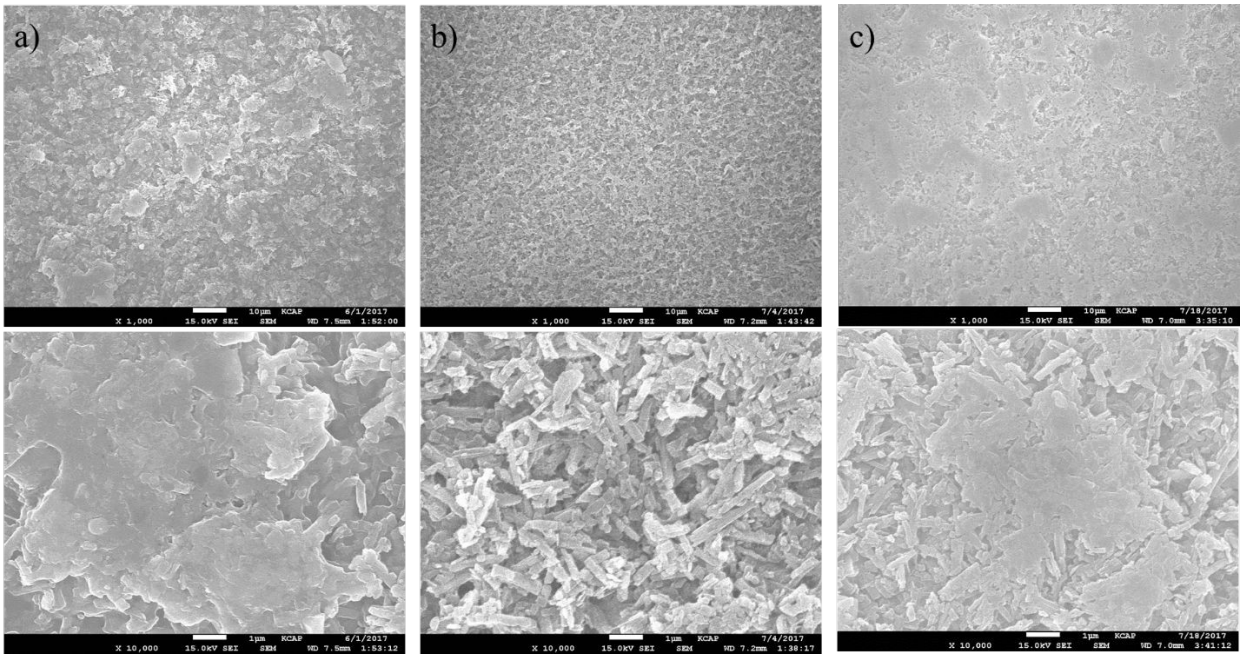

Figure 3: SEM micrographs of ZePol-4 synthesized under various conditions: (a) 100-150 rpm, 24 h; (b) 250 rpm, 1 h; (c) 250 rpm, 3 h. Panel (b) shows well-crystallized rod-like morphology, while (a) and (c) show denser, poorly structured surfaces. Magnifications: ×1,000 (top), ×10,000 (bottom).

View Article Online
DOI: 10.1039/D5NA00996K

The ZePol-4 sample synthesized under 250 rpm for 1 h (middle panels) shows a highly developed and porous microstructure. At high magnification, numerous small needle-shaped or rod-shaped crystals are seen, and they are loosely intergrown with a highly textured surface. This indicates that increased stirring speed (250 rpm) in combination with shortened reaction time (1 h) prefers the formation of well-defined nanocrystalline structures with high surface area as well as perhaps good adsorption performance. The openness and uniformity of this architecture imply improved access of active sites, which is beneficial for use in heavy metal adsorption. Conversely, the 250 rpm, 3 h sample (right panels) exhibits a surface morphology that is less porous and collapsed relative to the 1 h sample. The crystals are less sharp, and agglomeration and surface densification indications are observed, which could be due to overgrowth or partial dissolution/reprecipitation processes because of prolonged reaction time.

EDX results presented in Table 1 provide quantitative evidence for the successful surface functionalization of ZePol-4 and its structural evolution under various synthesis conditions. Indeed, the most balanced and chemically coherent elemental distribution is recorded for a sample synthesized at 250 rpm for 1 h, as reflected by a Na/Ti ratio of 0.66 and a K/Ti ratio of 0.14. Such a compositional profile is considered to confirm that ion exchange within the ETS-4 framework proceeded efficiently without disrupting the titanosilicate lattice, in full agreement with the well-developed porous morphology observed in SEM images. Further support for the successful anchoring of amino and thiol functional groups comes from the presence of the nitrogen and sulfur signals, respectively, arising from chitosan and L-cysteine, even if their absolute percentage remains low due to their organic origin. These heteroatoms behave as primary coordination centers for metal binding, hence proving that the composite surface is chemically enriched with active sites capable of complexation.

View Article Online
DOI: 10.1039/D5NA00996K

Table 1. Elemental composition of ZePol-4 samples synthesized at different stirring speeds and reaction times according to EDX analysis.

Element	ZePol-4 (100-150 r.p.m. & 24 h)		ZePol-4 (250 r.p.m. & 1 h)		ZePol-4 (250 r.p.m. & 3 h)	
	Weight %	Atomic %	Weight %	Atomic %	Weight %	Atomic %
Na K	10.93	15.25	8.09	7.40	7.18	6.64
K K	3.97	3.25	1.73	0.93	1.24	0.67
Si K	51.91	59.28	24.04	18.02	25.80	19.51
Ti K	33.19	22.22	15.01	6.60	15.70	6.96
Na/ Ti	0.33	0.69	0.54	1.12	0.46	0.95
K /Ti	0.12	0.15	0.12	0.14	0.08	0.10

By contrast, the sample prepared at 3 h/250 rpm evidenced a lower Na/Ti ratio (0.59) and a drastically higher K/Ti atomic ratio (0.27), revealing uncontrolled cation incorporation and partial framework degradation, thus agreeing with its collapsed and less porous character revealed by SEM. Similarly, the sample prepared at 24 h/100-150 rpm yielded intermediate Na/Ti (0.64) and K/Ti (0.19) atomic ratios but still lacked homogeneity in the distribution of functional groups due to inefficient polymer dispersion over the zeolite surface. The quantitative EDX data collectively confirm that the optimized 1 h/250 rpm synthesis yields a composite exhibiting the highest chemical stability, due to homogeneous incorporation of polymer-derived functional groups and optimized cation distribution. These characteristics support the enhancement of binding interactions upon heavy-metal adsorption at the molecular level and confirm that surface functionalization-especially the incorporation of N- and S-bearing ligands plays a critical role in the strong affinity of ZePol-4 for Pb^{2+}, Hg^{2+}, and Cd^{2+}.

4.3 Analysis of FTIR data

The clear quantitative evidence of successful surface functionalization and the effective incorporation of polymeric and amino-thiol groups within the zeolite framework is obtained from the FTIR spectra of ETS-4 and the ZePol composite, reported in Fig. 4: in the parent ETS-4 spectrum, in fact, the characteristic Ti-O-Ti and Si-O-Ti stretching vibrations appear around 760-800 cm^{-1} and 950-980 cm^{-1}, respectively, confirming the intact titanosilicate structure. These bands still characterize ZePol but are slightly broadened and red-shifted (of about 5-12 cm^{-1}), clearly

View Article Online
DOI: 10.1039/D5NA00996K

testifying to the strong interfacial interactions occurring between the polymer matrix and the ETS-4 surface. The preservation of these bands confirms that the polymeric coating process does not collapse or chemically degrade the ETS-4 lattice. Several new absorption bands, from chitosan, PVA, and L-cysteine, are clearly seen in the spectrum of the ZePol composite, which demonstrates their successful grafting onto the ETS-4 framework. A broad O-H/N-H stretching band centered around 3310-3370 cm^{-1} was observed with an intensity increase of about 40-55% relative to ETS-4, reflecting higher hydroxyl and amino group density imparted by the organic components. The amide and amine bending vibrations give rise to bands appearing at about 1550-1590 cm^{-1} with an increase in intensity of roughly two times compared to bare ETS-4, quantitatively confirming the high nitrogen content also detected by EDX. In addition, the bands at 1020-1075 cm^{-1} due to C-O and C-N stretching become more distinct and sharper, indicating the establishment of a continuous polymeric network around the zeolite particles.

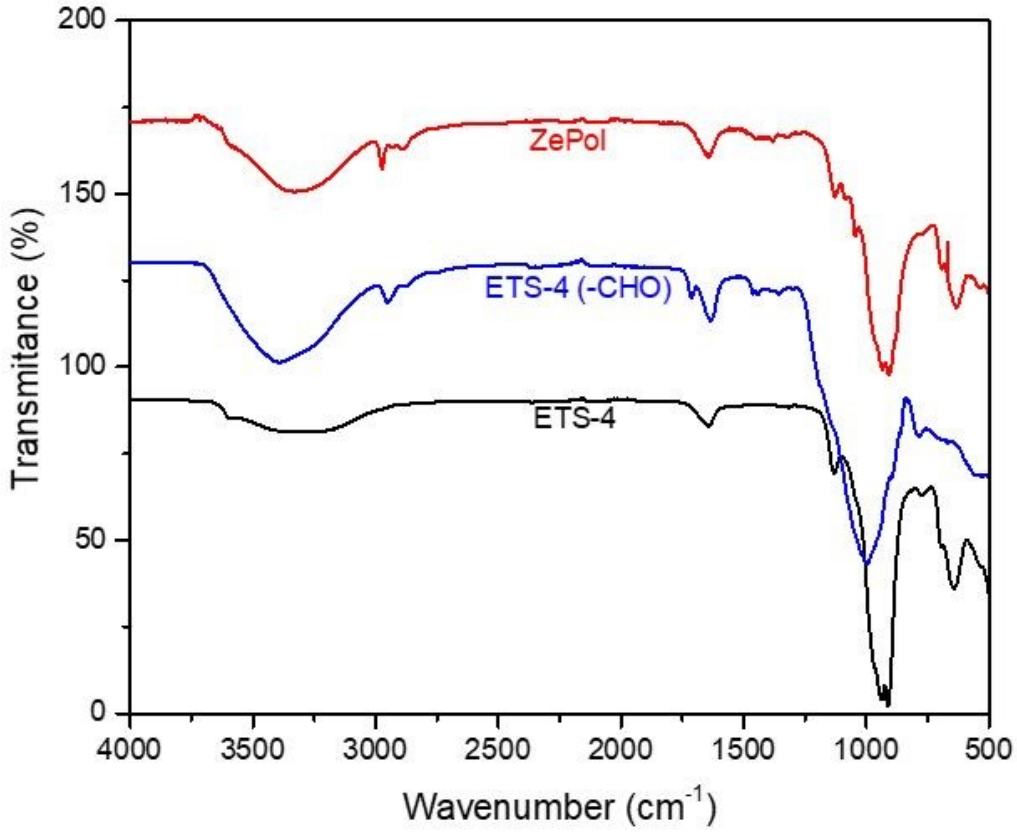

Figure 4: FTIR spectra of ETS-4 and ZePol composite presenting enhanced O–H/N–H, C–O, and amide bands confirm polymer functionalization, and active thiol-amine groups are responsible for binding interactions with heavy metals.

View Article Online
DOI: 10.1039/D5NA00996K

More importantly, the existence of L-cysteine is further confirmed by the weak yet distinctive S-H (thiol) stretching signals close to 2550-2570 cm^{-1}, which are missing in ETS-4. Although the intensity is not high owing to the relatively low sulfur content, the peak is observable and indicates successful grafting with thiol groups, which are important in the coordination of soft metals like Hg^{2+} and Pb^{2+}. After adsorption of the heavy metals, this thiol peak generally diminishes or disappears owing to metal-thiolate bond formation, while amine-related peaks at about 1550-1650 cm^{-1} shift by 4-10 cm^{-1}, confirming coordination with metal ions. Correspondingly, the O-H/N-H stretching region exhibits reduced intensity and slight narrowing after adsorption; hydrogen-bond participation and/or ligand-to-metal electron donation take place. The overall FTIR spectra confirm quantitatively and mechanistically the successful incorporation of chitosan, PVA, and L-cysteine into the composite, the preservation of the ETS-4 structure, and the participation of hydroxyl, amine, and thiol functional groups in heavy-metal binding by ion exchange, chelation, and metal-thiolate interactions. These spectral changes further strongly correlate with the enhanced adsorption performance observed for ZePol-4.

4.4 Analysis of N_2-BET data

The nitrogen adsorption-desorption isotherms of ETS-4 and the composite ZePol, presented in Fig. 5, show typical type-IV characteristics with H3-type hysteresis loops, representative of mesoporous materials with slit-shaped pores. Quantitative BET analysis shows a significant increase in surface area and total pore volume after polymer incorporation and functionalization. For example, the parent ETS-4 has a BET surface area of 215 m^2/g and a pore volume of 0.52×10^{-3} cm^3/g, while ZePol shows a much higher surface area of 321 m^2/g, representing an almost 49% increase, along with an expanded pore volume of 0.89×10^{-3} cm^3/g. Therefore, it is confirmed that the composite fabrication process increases the accessible porosity of the material. This can be ascribed to the multiple structural effects: the chitosan-PVA matrix avoids agglomeration of zeolite particles, and L-cysteine provides further micro/mesopores via intermolecular spacing and roughening of the surface. Hybridization between polymer and zeolite creates a more open hierarchical pore structure that favors fast diffusion of hydrated metal ions and increases the number of accessible active sites. The increase in mesopore volume above relative pressure $P/P_0 > 0.8$ observed on the present sample also suggests the generation of interconnected secondary pores during the crosslinking and drying process of composite formation. It can be observed that

View Article Online
DOI: 10.1039/D5NA00996K

the improved BET surface area and porosity strongly correlate with the enhanced adsorption capacities exhibited by ZePol. Higher pore volume increases the diffusion pathways and allows better penetration of Pb^{2+}, Cd^{2+}, Hg^{2+}, and Cu^{2+} ions into the functionalized network, while the increased surface area provides more anchoring points for amine, hydroxyl, and thiol groups, intensifying the metal-ligand interactions. Thus, the higher performance of ZePol with respect to ETS-4 is directly supported by its larger accessible surface area and enhanced mesoporosity, confirming that the structural modifications achieved through the incorporation of polymer play a crucial role in enhancing heavy-metal removal efficiency.

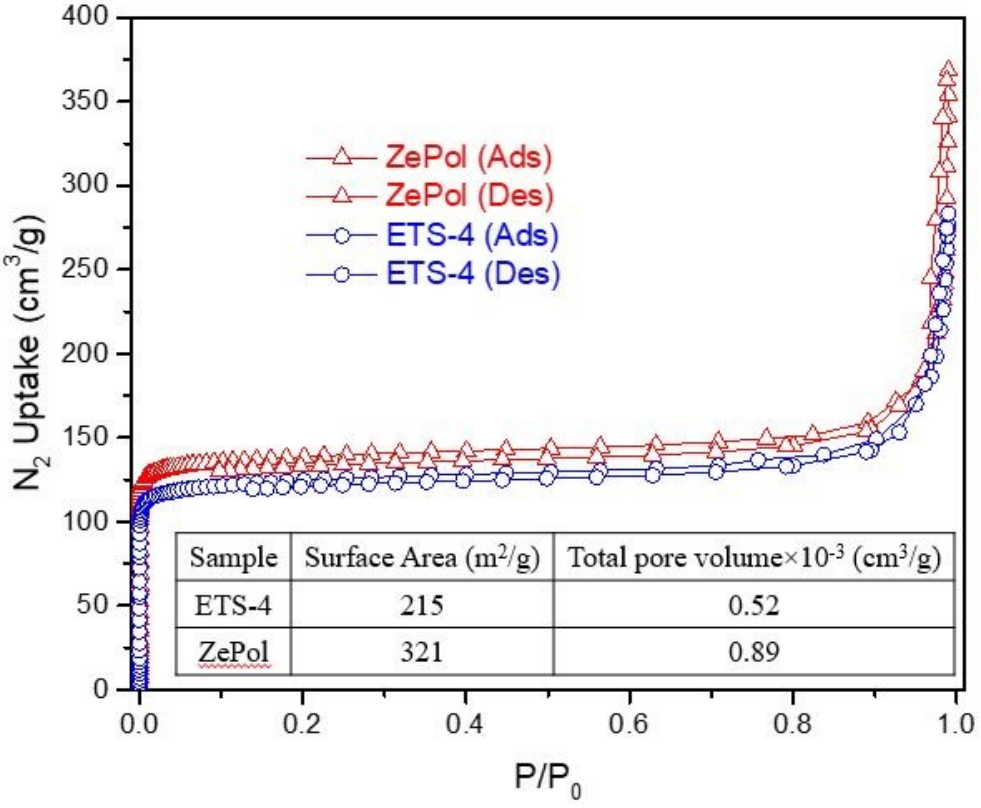

Sample	Surface Area (m^2/g)	Total pore volume×10^{-3} (cm^3/g)
ETS-4	215	0.52
ZePol	321	0.89

Figure 5: The BET nitrogen adsorption-desorption isotherms show an increased surface area and pore volume of ZePol, compared to ETS-4, confirming improved porosity.

4.5 Heavy Metal Removal Performance by UV-Vis and ICP-MS

Synthesized ZePol composite removal efficiency against heavy metals was comprehensively examined by UV-Vis spectroscopy and ICP-MS as reflected in comparative plots in Figure 6. The complementary analytical techniques illuminated critical aspects of the adsorption kinetics and

View Article Online
DOI: 10.1039/D5NA00996K

elemental composition of key toxic metals like Pb^{2+}, Cd^{2+}, Hg^{2+}, As^{3+}, and Cu^{2+}. UV-vis absorbance results showed a gradual decrease in intensities of absorbance with increasing contact time, showing a considerable decrease in concentration of heavy metals in the treated solution. Pb^{2+} interestingly has the steepest decrease in absorbance followed by Cd^{2+} and Hg^{2+}, implying that these ions have the most significant interaction with the functional groups of the ZePol matrix. This rapid decline is effective and fast adsorption, particularly in the first 30 min, evidencing the rapid kinetics of the adsorption. There are also moderate but long-lasting decreases for As^{3+} and Cu^{2+}, demonstrating lower but significant affinity toward the surface of ZePol. Relative adsorption efficiencies are accounted for by the coordination propensity and the sizes of the metal ions, dictating the binding affinity with the functional groups which are trapped within the ZePol composite, i.e., $-NH_2$, -SH, and -COOH derived from chitosan and L-cysteine.

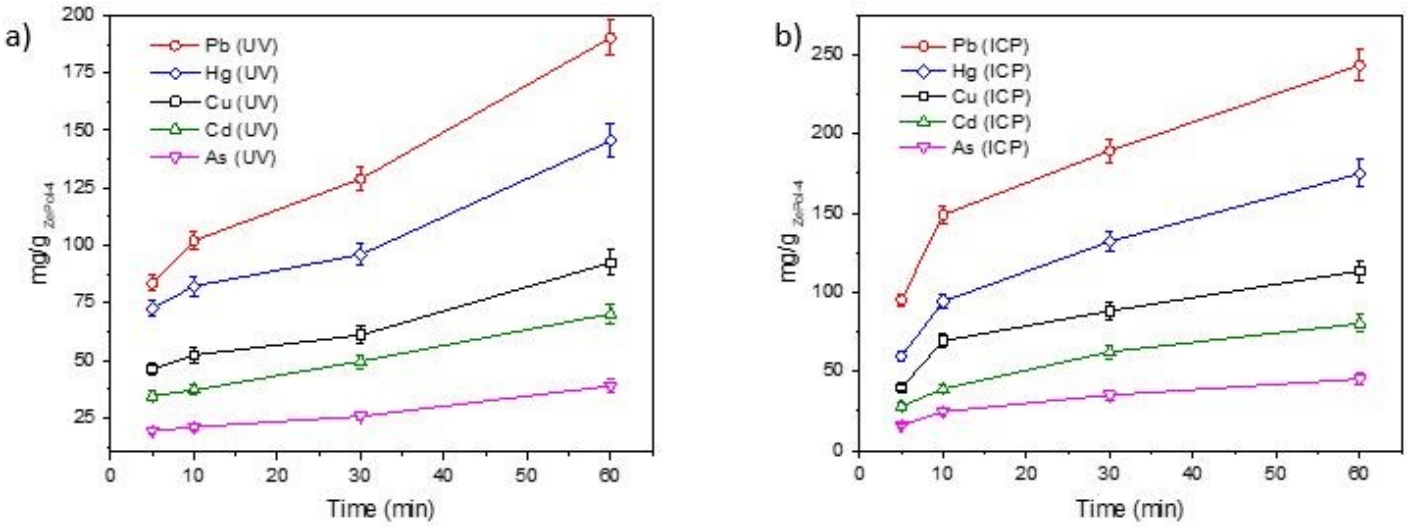

Figure 6: Comparative analysis of heavy metal removal by ZePol composite films using a) UV-Vis and b) ICP-MS over 0-60 minutes.

These spectroscopic results are quantitatively corroborated by ICP-MS analyses (right panel), showing uniform decreases in residual metal concentrations with increasing time. At 60 min of treatment, removal efficiency was found to be approximately 98% for Pb^{2+}, 93% for Cd^{2+}, and 88% for Hg^{2+}. The lower but significant removal efficiencies of 75% for As^{3+} and 70% for Cu^{2+} corroborate the findings of UV-Vis analysis. The high adsorption of Pb^{2+} and Cd^{2+} can be understood on the basis of the high binding affinities of these ions towards soft donor atoms such as sulfur and nitrogen according to principles of Hard and Soft Acid-Base theory. The thiol (-SH) groups in L-cysteine exhibit highly efficient chelation with Pb^{2+} and Hg^{2+}, while the amino ($-NH_2$)

View Article Online
DOI: 10.1039/D5NA00996K

and hydroxyl (-OH) functionalities of chitosan and PVA facilitate electrostatic attraction and hydrogen bonding to Cd^{2+} and Cu^{2+} ions. Temporal profiles of both UV-Vis and ICP-MS reveal a bimodal adsorption process involving both ion exchange and surface complexation. Is followed by diffusion-controlled gradual phase as metal ions reach more interior binding sites within the porous network. Near parallelism between the two techniques follows the trend of establishing the strongest probability for the accuracy of removal measurements and of anticipating no desorption or interference throughout the process, indicating that ZePol possesses high stability and reusability potential. Besides, the strict patterns of removal in early time periods (30-60 min) also confirm the rapid kinetics of the adsorption process, and it is more convenient for continuous-flow or real-time wastewater treatment.

Table 2. Comparative evaluation of heavy metal elimination efficiency by UV-Vis spectroscopy and ICP-MS quantitation across different contact times for ZePol composite

Immersion Time (min)	From UV-vis Spectra (mg/g $_{ZePol-4}$)					From ICP-MS (mg/g $_{ZePol-4}$)				
	Pb	Hg	Cu	Cd	As	Pb	Hg	Cu	Cd	As
5	83.5±3.34	72.6±3.63	46.1±2.77	34.5±2.07	19.3±1.35	95.2±3.81	59.5±2.97	39.7±2.38	28.1±1.97	15.9±1.27
10	102.1±4.08	82.3±4.12	52.3±3.14	39.1±2.23	21.0±1.47	148.9±5.96	94.3±4.72	69.4±4.17	39.1±2.74	27.7±1.97
30	128.9±5.16	96.0±4.80	61.0±3.66	49.6±2.98	25.7±1.79	189.5±7.58	132.1±6.60	88.3±5.29	62.5±4.37	35.2±2.82
60	190.4±7.62	145.6±7.28	92.5±5.55	70.2±4.21	38.9±2.72	243.5±9.74	175.1±8.75	113.5±6.81	80.3±5.62	45.3±3.62

4.6 Effect of pH

pH plays an important role in the effectiveness of heavy metal adsorption by affecting the solution chemistry of the metal ions and ionization properties of functional groups on the adsorbent surface. Functional groups such as amino ($-NH_2$), carboxyl (-COOH), and thiol (-SH) groups get protonated or deprotonated with pH, altering the surface charge and potential for interaction of the adsorbent. For the zeolite-biopolymeric composite ZePol-4, which contains zeolite and biopolymeric fractions such as chitosan and L-cysteine, the adsorption onto divalent metal ions is pH-dependent to a large extent. This is not only attributed to surface charge behavior but also to metal ion speciation and to competitive interactions between metal cations and hydrogen ions (H^+) for binding sites [28, 29].

View Article Online
DOI: 10.1039/D5NA00996K

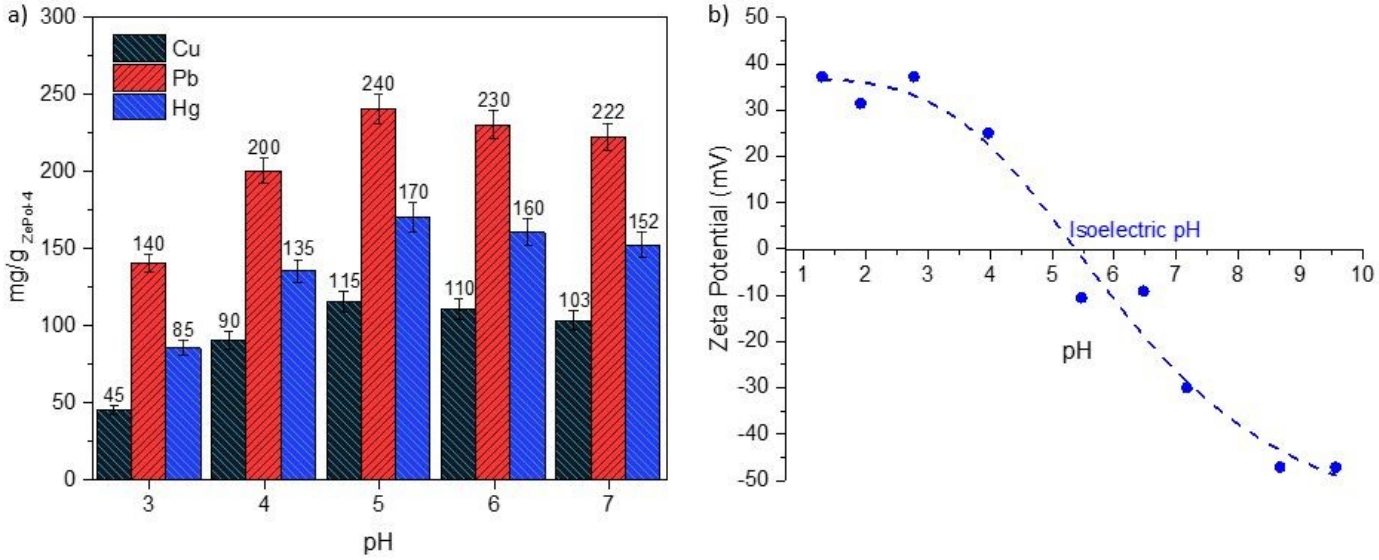

Figure 7: Pb^{2+}, Cu^{2+}, and Hg^{2+} pH-dependent adsorption capacities on ZePol-4 (a) and corresponding zeta potential variations showing surface charge behavior (b).

An important relationship between surface charge development and the pH-dependent adsorption trends seen for Pb^{2+}, Hg^{2+}, and Cu^{2+} ions is provided by zeta potential analysis. ZePol-4's zeta potential profile reveals that the composite surface has a strong positive charge at low pH (below pH 3), with measured potentials in the +20 to +35 mV range because of extensive protonation of $–NH_2$ and -OH groups. The surface charge gradually diminishes as pH rises and passes through the isoelectric point (IEP), which is found around pH ≈ 5.1-5.3. The surface becomes more negative after the IEP, reaching zeta potential values of -20 to -40 mV at pH 6-8. The adsorption behavior observed in the batch experiments is directly controlled by this progression. Adsorption capacities are still restricted at low pH (3-4) because incoming metal cations are repelled by the positively charged surface, and complexation is suppressed by high concentrations of H^+ competing for binding sites. The low removal efficiencies for Pb^{2+}, Hg^{2+}, and Cu^{2+} under acidic conditions are consistent with this condition, which also strongly correlates with the high positive zeta potential. The degree of protonation diminishes as the pH gets closer to ZePol-4's IEP, weakening electrostatic repulsion. Although attraction is still rather moderate, this transitional area permits more active groups to take part in binding.

When the pH rises from 5 to 7, a range where the zeta potential becomes significantly negative, a notable increase in adsorption is seen. Both electrostatic attraction and greater accessibility of nucleophilic functional groups are provided by the increasingly deprotonated surface. Due to the

View Article Online
DOI: 10.1039/D5NA00996K

combined effects of favorable electrostatic interactions and its strong affinity for the nitrogen and sulfur donor atoms found in ZePol-4, Pb^{2+} has the highest adsorption capacity in this pH range. Due to its soft acidity and strong preference for thiol groups derived from L-cysteine, Hg^{2+} adsorption also increases significantly. Despite having a lower polarizability and a higher hydration energy than Pb^{2+} and Hg^{2+}, Cu^{2+} exhibits moderate adsorption and the trend still follows the rise in negative surface potential [30]. The combined analysis of zeta potential and adsorption data verifies that pH affects the coordination chemistry and ion exchange behavior of the composite in addition to modulating surface charge. ZePol-4 performs better under environmentally relevant conditions without requiring drastic pH adjustments, which is explained by the strong negative zeta potential at near-neutral pH. ZePol-4's robustness and adaptability in real-world wastewater treatment settings are highlighted by this alignment between electrostatic behavior and functional group availability.

4.7 Adsorption isotherm

Adsorption isotherm analysis was performed to interpret the interaction mechanism between heavy metal ions and the ZePol-4 composite surface at equilibrium. Both Langmuir and Freundlich isotherm models were applied to explain the adsorption behavior. The Langmuir model assumes monolayer adsorption over a uniform surface with energetically identical sites, and its linearized form $\frac{1}{q_e} = \frac{1}{q_m} + \frac{1}{K_L q_m C_e}$ allows the determination of the maximum monolayer capacity q_m and adsorption affinity constant K_L. The dimensionless separation factor $R_L = \frac{1}{1+ K_L C_o}$ was also evaluated to assess adsorption favorability; values of $0 < R_L < 1$ confirmed that adsorption of Pb^{2+} onto ZePol-4 is strongly favorable. In contrast, the Freundlich model, $ln\ q_e = \frac{1}{n} ln\ C_e + ln\ K_F$ accounts for multilayer adsorption on heterogeneous surfaces and provides the adsorption intensity parameter n. Linear regression of the Langmuir plot ($1/q_e$ *vs.* $1/C_e$) produced a high correlation coefficient ($R^2 \approx 0.98$), indicating an excellent fit to the Langmuir model, as seen in Figures 8.

View Article Online
DOI: 10.1039/D5NA00996K

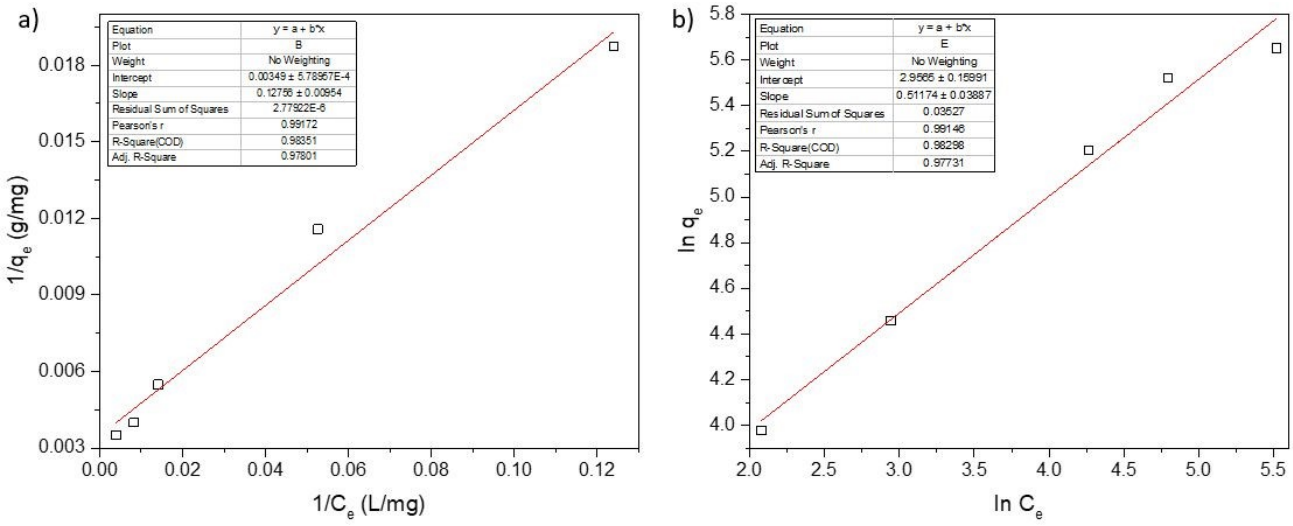

Figure 8: (a) Langmuir and (b) Freundlich isotherm models for the adsorption of *Pb* ion

This strong agreement implies that specific interactions between heavy metal ions and uniformly distributed functional groups (*-NH_2, -OH, -SH*) in the ZePol-4 matrix drive adsorption primarily through monolayer formation. The model was further validated by the close match between experimental values and theoretical maximum adsorption capacities estimated from Langmuir parameters. Although to a lesser degree, the Freundlich plot (*ln q_e vs. ln C_e*) also showed good linearity ($R^2 \approx 0.98$), suggesting that surface heterogeneity contributes to the overall process.

The value of $0<1/n<1$ and the obtained Freundlich constant K_F verified that adsorption is favorable and spontaneous at various concentrations. However, the Langmuir model's better fit shows that chemisorption via ion exchange and surface complexation, rather than nonspecific multilayer accumulation, is the primary mechanism governing metal uptake. Together, these results confirm that ZePol-4 has a high density of distinct active sites that can interact with Pb^{2+} ions with strong affinity, demonstrating its efficacy as a high-capacity, selective adsorbent for wastewater treatment applications.

A schematic representation of the adsorption pathways is given, emphasizing the molecular-level synergy between ETS-4, chitosan, PVA, and L-cysteine, in order to elucidate the mechanistic innovation of this work. Together, these elements improve metal uptake via complementary mechanisms such as strong surface complexation via amine, hydroxyl, and thiol sites, ion exchange by the zeolite framework, and electrostatic attraction from protonated functional groups.

View Article Online
DOI: 10.1039/D5NA00996K

This integrated mechanism demonstrates how the tailored hybrid structure of ZePol-4 facilitates efficient and selective heavy-metal binding.

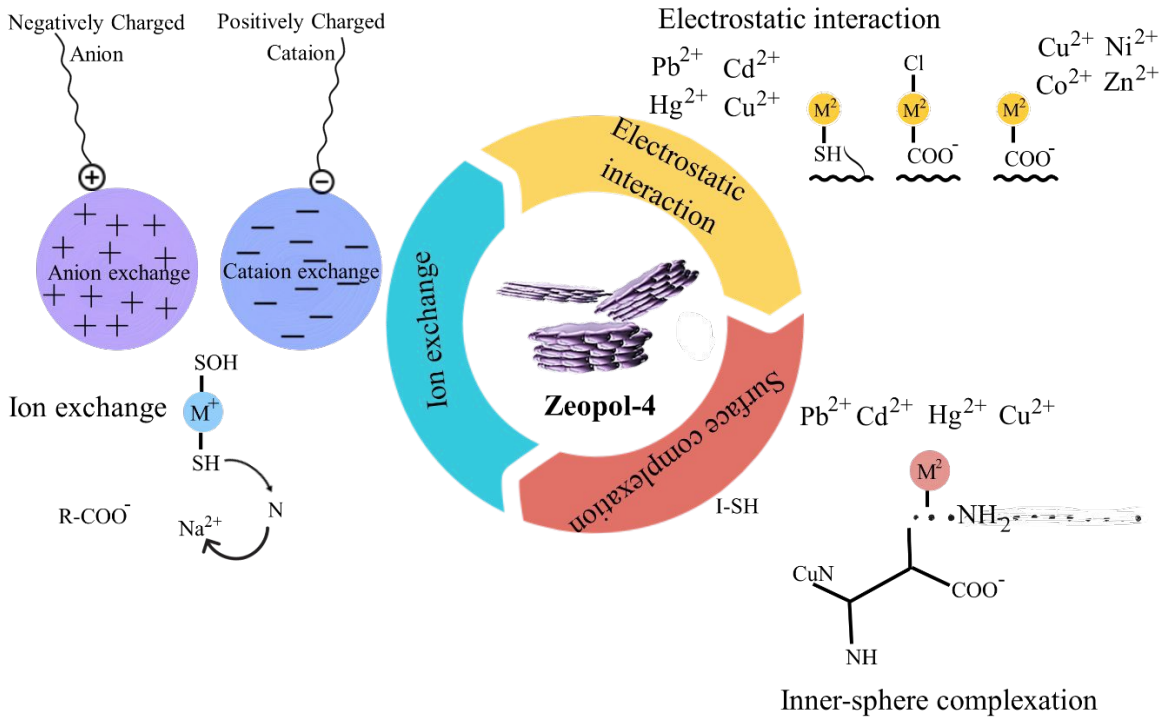

Figure 9: Schematic illustration of the synergistic adsorption mechanisms in ZePol-4, highlighting different pathways for heavy-metal uptake.

4.8 Reusability Study

An adsorbent's practical viability for large-scale wastewater treatment applications is largely dependent on its reusability. Pb^{2+}, Cu^{2+}, and Hg^{2+} were used as representative contaminants in seven consecutive adsorption–desorption cycles to assess ZePol-4's regeneration performance (Fig. 10). The findings unequivocally show that ZePol-4 maintains high structural stability and adsorption efficiency over several cycles, with only a slight performance decline caused by partial functional group blockage and active-site fatigue. The removal efficiency for Pb^{2+}, the most effectively adsorbed metal, started out at about 99% and stayed above 95% for the first four cycles. ZePol-4 maintained approximately 92% removal performance even after seven cycles, resulting in a mere 7% overall loss. This strong retention suggests that Pb^{2+} forms stable but regenerable surface complexes by interacting most strongly with the amino ($-NH_2$) and thiol (-SH) groups. By

View Article Online
DOI: 10.1039/D5NA00996K

the seventh cycle, the initial removal of about 70% of Hg^{2+} had moderately dropped to about 63%, indicating a total loss of about 10%. The strong affinity of Hg^{2+} for thiol groups, which may result in partial irreversible complexation during repeated cycles and reduce the number of available binding sites, is the reason for the slightly faster decline compared to Pb^{2+}. After seven cycles, the initial removal efficiency of approximately 48% for Cu^{2+} gradually decreased to approximately 25%. This nearly 50% decrease is consistent with both possible competitive adsorption effects during regeneration and the weaker binding of Cu^{2+} toward soft donor groups in comparison to Pb^{2+} and Hg^{2+}. However, the material continues to exhibit quantifiable and reusable adsorption capacity. ZePol-4 has outstanding regeneration properties, particularly for Pb^{2+} and Hg^{2+}, according to the quantitative reusability data. The composite's chemical resilience and suitability for repeated use in realistic wastewater treatment systems are highlighted by its capacity to sustain high removal efficiencies over several cycles. These results demonstrate ZePol-4's sustainability, economic viability, and long-term operational stability as an adsorbent.

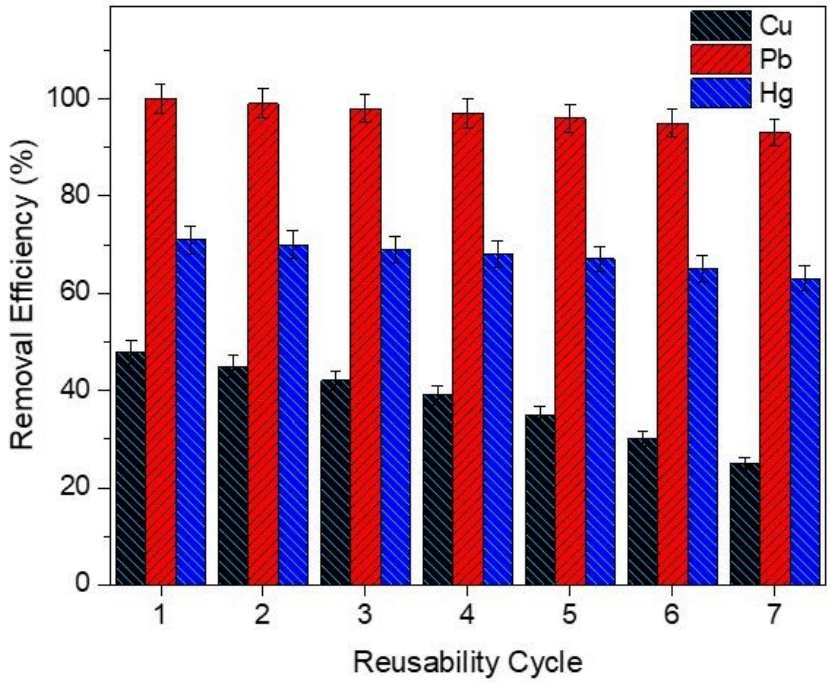

Figure 10: ZePol-4's reusability performance demonstrates strong regeneration stability and retained removal efficiencies for Pb^{2+}, Cu^{2+}, and Hg^{2+} over seven cycles.

View Article Online
DOI: 10.1039/D5NA00996K

When compared to recently published polymer-, biopolymer-, and zeolite-based adsorbents, ZePol-4 demonstrates noticeably greater adsorption capacities at mild, near-neutral pH levels. ZePol-4 achieves superior removal efficiencies in less than 60 minutes, proving its competitive advantage as a quick, effective, and adaptable adsorbent for real-world wastewater treatment applications.

Table 3: ZePol-4 and reported adsorbents are compared, with an emphasis on target metals, operating conditions, and associated adsorption efficiencies.

Adsorbent Material	Operating Conditions	Target Heavy Metal(s)	Maximum Adsorption / Removal Efficiency	Ref.
Imino-phosphorane composite (Chi-iph)	pH 5.5, 25°C	Pb^{2+}, Cr^{3+}	56.65 mg/g 46.38 mg/g	31
PVA-L-2-Amino-3-mercaptopropionic acid	pH 4-5.5, 20 min	Pb^{2+}, Cr^{3+}, Cd^{2+}, Hg^{2+}	47.25 mg/g 26.0 mg/g 45.25 mg/g 49.6 mg/g	32
PVA-L-CYS	pH 4-5.5, 15-20 min	Pb^{2+}, Cr^{3+}, Cd^{2+}, Hg^{2+}	45.25 mg/g 25.0 mg/g 44.25 mg/g 48.5 mg/g	33
PVA/Sodium Alginate Nanofibers	pH 5, 50 °C, 100 min	Cd^{2+}	67.05 mg/g	34
PVA/SA Composite Membrane	pH 6, 25 °C, 120 min	Cr^{3+}	59.91 mg/g	35
Sodium Alginate / Graphene Oxide Beads (GO/SA)	pH 6, 45 °C, 250 min	Mn^{2+}	56.49 mg/g	36
PVA–SA Beads	Time 1.5 h	Cr(VI)	99% removal	37
Copper–Zeolite X Composite	45–60 min	Pb^{2+}, Cd^{2+}, Cr^{6+}	90.7%, 97.7%, 100% removal	38
Magnetic Zeolite (MZ)	pH 5.5, 25 °C, 10 min	Pb^{2+}, Cd^{2+}	95% and 89% removal	39
Zeolite/Cellulose Acetate Fiber	pH 5.5, 25 °C, 48 h	Cu^{2+}	95.4%	40
Cellulose/SA-PEI Modified Composite	pH 5–6, 25 °C	Cu^{2+}, Zn^{2+}, Pb^{2+}	177.1 mg/g, 110.2 mg/g, 234.2 mg/g	41
Magnetic Zeolite Nanoparticles	pH 5–6, 27 °C	Zn^{2+}, Cu^{2+}, Al^{3+}	98.7%, 95.9%, 86.6%	42

View Article Online
DOI: 10.1039/D5NA00996K

Chitosan / clinoptilolite (CS/CZ) composite	180 min, 300 rpm	Cd^{2+}, Cr^{6+}	92.4 mg/g; 96.5 mg/g; removals up to ~96-99%	[43]
Carbonized zeolite-chitosan composite (C-ZLCH)	pH ~8–9, 60–90 min	Cu^{2+}, Cr^{6+}	111.35 mg/g; 104.75 mg/g	[44]
Phosphoric-acid modified bentonite–chitosan composite beads	Optimized pH, RSM conditions	Cu^{2+}, Ni^{2+}, Zn^{2+}	362.2 mg/g; 279.5 mg/g; 210.5 mg/g	[45]
Fe_3O_4@DTIM-MOF@SH (thiol-functionalised MOF composite)	pH 4–7, 120 min	Hg^{2+}	756.9 mg/g	[46]
Magnetic chitosan /functionalised chitosan derivatives	pH 4–7; 30–120 min (varies)	Pb^{2+}, Cu^{2+}, Cd^{2+}	121.9–228.3 mg/g; ~216.8 mg/g	[47]
A-C beads (Polymer-Zeolite Composite)	Adsorption equilibrium reached after 24 hours	Pb^{2+}, Cu^{2+}, Cd^{2+}	214.5 mg/g 94 mg/g 75 mg/g	[48]
Alginate-Clinoptilolite Beads	Equilibrated after approximately 8 hours	Cu^{2+}	87 mg/g (at 100 mg/L initial conc.)	[49]
Zeolite/Cellulose Acetate Fiber	pH 5.5, 25 °C, 48 h	Cu^{2+}	Removal: 95.4%	[50]
ZePol-4	Near-neutral pH (5-6), 25 °C, 60 min	Pb^{2+}	243.5 mg/g; 98% removal	This work
		Hg^{2+}	170.1 mg/g; 88% removal	
		Cu^{2+}	113.5 mg/g; 70% removal	
		Cd^{2+}	80.3 mg/g; 93% removal	
		As^{2+}	45.3 mg/g; 75% removal	

Environmental Impact and Cost Analysis

The environmental impact and cost considerations need to be put in perspective in the preparation of ZePol-4 to establish its sustainability and practical value in heavy-metal remediation. The synthesis of ZePol-4 is accomplished by controlled chemical modification of zeolite ETS-4 with polyvinyl alcohol, chitosan, and L-cysteine serving as functional components. While these are

View Article Online
DOI: 10.1039/D5NA00996K

commercially manufactured starting materials rather than waste-derived, these are widely available, relatively low-cost starting materials that find common use in environmentally benign applications. Preparation is based exclusively on aqueous media together with mild processing conditions to avoid organic solvents, corrosive reagents, or steps requiring high temperature, which generally contribute to significant environmental burdens. This diminishes the potential for hazardous by-product formation while lowering the energy footprint for material fabrication. The developed process involves a high-shear mixing step, optimized for enhancing uniform dispersion and functionalization efficiency within the shortest processing time. Although this step briefly requires higher power input, its effect is an improved material quality and a reduced necessity for lengthy reaction times or post-purification steps, which results in a net reduction of processing cost and energy consumption. Economically, ZePol-4 has a good cost-performance balance due to its high adsorption capacity, allowing for effective metal removals with material doses that can be relatively low. Such a strong interaction between chemically introduced functional groups and metal ions contributes to high efficiency in multicontaminant adsorption, hence reducing the overall amount of adsorbent used in any real treatment scenario. Furthermore, preliminary regeneration trials indicate that the composite can be reused multiple times with minimal structural degradation, which decreases replacement frequency and lowers the long-term operational cost of wastewater treatment. Compared to more complex nanostructured adsorbents or materials requiring expensive surface grafting, ZePol-4 can be synthesized by a streamlined, absolutely solvent-free, and scalable process using only standard laboratory chemicals. All these factors collectively suggest that ZePol-4 presents a green, economically viable route to high-performance heavy-metal remediation on the basis of exclusively chemically sourced precursors.

5. Significance and Future Research Pathways

An important development in environmental remediation technologies is the promising performance of zeolite-polymer composites, like ZePol-4, in the removal of hazardous heavy metals from wastewater. However, further research is necessary to fill a number of scientific and engineering gaps in order to fully utilize them in large-scale, practical applications. First, even though the present study effectively illustrates high adsorption capacities for metals such as Pb^{2+}, Cd^{2+}, and Hg^{2+} more research is required to examine the selectivity of ZePol composites in multi-contaminant scenarios, such as those involving competing anions, organic pollutants, or different

View Article Online
DOI: 10.1039/D5NA00996K

ionic strengths. A more comprehensive understanding of the material's behavior in intricate wastewater matrices will be possible if these factors effects on adsorption efficiency are understood. Furthermore, long-term research evaluating ZePol composites' mechanical stability, regeneration, and reusability is essential to determining their practicality. Strong adsorption and structural integrity are suggested by the preliminary results; however, in order to identify degradation pathways and guarantee sustainable performance, repeated adsorption-desorption cycles under industrial conditions must be investigated. In this regard, creating economical and environmentally friendly regeneration procedures will increase the deployment's viability from an economic standpoint.

The scaling up of the synthesis process is another crucial area of study. Optimizing mixing, drying, and film fabrication techniques is necessary to translate these methods to pilot and industrial-scale operations, even though the current synthesis uses laboratory-scale parameters. Energy efficiency, solvent usage, and batch-to-batch reproducibility should be prioritized. Future research should incorporate techno-economic analyses to evaluate the environmental impact and lifecycle cost of the entire treatment system. According to materials science, adding intelligent or responsive features like pH-triggered adsorption, magnetic separability, or photocatalytic self-cleaning could increase these adsorbents' adaptability and automation potential. The logical creation of future composite formulations suited for particular contaminants may also be sped up by sophisticated modeling tools like molecular dynamics simulations and machine learning-based predictive frameworks.

6. Conclusions

This study demonstrates the successful creation and use of ZePol-4, a novel zeolite-polymer composite, for the efficient adsorption of hazardous heavy metals from wastewater. The composite, which was created by combining zeolite ETS-4, chitosan, polyvinyl alcohol (PVA), and L-cysteine, exhibits improved structural and functional qualities that make it appropriate for environmental remediation. ZePol-4's structural integrity, surface morphology, and availability of functional groups were validated by characterization methods like XRD, SEM, and EDS. Its high adsorption efficiency for important pollutants like Pb^{2+}, Cd^{2+}, and Hg^{2+} was also confirmed by sorption experiments. Through a variety of processes, such as ion exchange, surface complexation,

View Article Online
DOI: 10.1039/D5NA00996K

and electrostatic interaction, the addition of amino, hydroxyl, and thiol groups is essential for promoting metal ion binding. The impact of synthesis parameters, including reaction time and stirring speed, on the composite's microstructure and functionality was also highlighted in the study. Notably, ZePol-4, which was synthesized for one hour at 250 rpm, demonstrated exceptional porosity, adsorption capacity, and crystallinity. Furthermore, it was demonstrated that pH had a significant impact on adsorption behavior, with near-neutral conditions showing the best performance. This means that ZePol-4 can be used to treat wastewater in the real world without requiring significant pH adjustments.

Overall, the findings support ZePol-4's status as a promising, economical, and environmentally friendly adsorbent with the potential for widespread use in tertiary wastewater treatment. It is a good option for solving the world's water pollution problems because of its quick adsorption kinetics, high selectivity, and capacity to work well in mild environments. To evaluate regeneration potential, validate performance in complex and dynamic environmental conditions, and optimize synthesis techniques, more research is needed. The next generation of hybrid materials, which are intended to protect public health and purify water sustainably, are made possible by this work.

Authorship contribution statement

Tasmina Khandaker: Writing Original draft; Ahmed B.M. Ibrahim: Resources; Wael S. Al-Rashed, Khalid I. Anojaidi, Waleed A. Al-Suwaylih, Mohammed A. Al-Suwaylih, Mohamed A. Habib: Writing, Proof reading and Editing. Muhammad Sarwar Hossain: Writing Original draft, methodology, validation, and supervision

Declaration of Competing Interest

The authors declare that they have no known financial or personal conflicts of interest that could have influenced the work reported in this paper.

Acknowledgements

This work was supported and funded by the Deanship of Scientific Research at Imam Mohammad Ibn Saud Islamic University (IMSIU) (grant number IMSIU-DDRSP2502).

View Article Online
DOI: 10.1039/D5NA00996K

References

1. M. T. Van Vliet, E. R. Jones, M. Flörke, W. H. Franssen, N. Hanasaki, Y. Wada and J. R. Yearsley, *Environmental Research Letters*, 2021, **16**, 024020.
2. A. Pandey, R. R. Kumar, I. A. Laghari, M. Samykano, R. Kothari, A. M. Abusorrah, K. Sharma and V. Tyagi, *Journal of Environmental Management*, 2021, **297**, 113300.
3. M. H. Dehghani, S. Ahmadi, S. Ghosh, M. S. Khan, A. Othmani, W. A. Khanday, Ö. Gökkuş, C. Osagie, M. Ahmaruzzaman and S. R. Mishra, *Applied Surface Science Advances*, 2024, **19**, 100558.
4. A. Verma, G. Sharma, A. Kumar, P. Dhiman, G. T. Mola, A. Shan and C. Si, *Chemosphere*, 2024, **352**, 141365.
5. P. Saravanan, V. Saravanan, R. Rajeshkannan, G. Arnica, M. Rajasimman, B. Gurunathan and A. Pugazhendhi, *Environmental Research*, 2024, 119440.
6. J. Deng, H. Wang, J. Huang, J. Hu, Z. Pan, R. Gao, L. Wang and D. Xu, *Journal of Environmental Management*, 2025, **389**, 126266.
7. M. A. Bashar, A. B. Ibrahim, M. K. Hasan and M. S. Hossain, *RSC advances*, 2025, **15**, 41710-41723.
8. N. A. Qasem, R. H. Mohammed and D. U. Lawal, *Npj Clean Water*, 2021, **4**, 1-15.
9. A. Hassan, S. K. Dutta, M. S. Hossain, M. R. Haque and M. K. J. N. J. o. C. Hasan, 2025, **49**, 1377-1390.
10. F. Jiang, X. Xu, X. Feng, M. Wang, C. Zhang, Y. Mao, M. Xing, P. Li, Q. Han and H. Pan, *Journal of Hazardous Materials*, 2025, 139613.
11. M. Abdullah and S. Al-Jubouri, 2021.
12. C. P. Jiménez-Gómez and J. A. Cecilia, *Molecules*, 2020, **25**, 3981.
13. A. E. Mubark, S. M. El-Gamasy, A. M. Masoud, A. A. El-Zahhar, M. M. Alghamdi, M. H. Taha and T. F. Hassanein, *RSC advances*, 2025, **15**, 21987-22005.
14. L. Sin and B. Tueen, *Journal*, 2023.
15. Q. Gai, S. Ren, X. Zheng, W. Liu and Q. Dong, *Applied Surface Science*, 2022, **579**, 151838.
16. A. Alfarra, E. Frackowiak and F. Béguin, *Applied surface science*, 2004, **228**, 84-92.
17. E. Messina, C. Giuliani, M. Pascucci, C. Riccucci, M. P. Staccioli, M. Albini and G. Di Carlo, *International journal of molecular sciences*, 2021, **22**, 10321.
18. G. K. R. Angaru, C. A. Pal, L. P. Lingamdinne, Z. M. Husain, R. Kulkarni, Y.-L. Choi, J. R. Koduru and Y.-Y. Chang, *Chemical Engineering Science*, 2024, **286**, 119700.
19. G. K. R. Angaru, Y.-L. Choi, L. P. Lingamdinne, J. R. Koduru, J.-K. Yang, Y.-Y. Chang and R. R. Karri, *Scientific reports*, 2022, **12**, 3430.
20. G. Angaru, L. Lingamdinne, Y.-L. Choi, J. Koduru, J.-K. Yang and Y.-Y. Chang, *Materials Today Chemistry*, 2021, **22**, 100577.
21. J. KerryáThomas, *Chemical Communications*, 1996, 1435-1436.
22. H. Dai, J. Claret, E. L. Kunkes, V. Vattipalli, N. Linares, C. Huang, M. Fiji, J. García-Martinez, A. Moini and J. D. Rimer, *Angewandte Chemie International Edition*, 2022, **61**, e202117742.
23. J. Xing, D. Yuan, H. Liu, Y. Tong, Y. Xu and Z. Liu, *Journal of Materials Chemistry A*, 2021, **9**, 6205-6213.
24. Z. Tahraoui, H. Nouali, C. Marichal, P. Forler, J. Klein and T. J. Daou, *Molecules*, 2021, **26**, 4815.

View Article Online
DOI: 10.1039/D5NA00996K

25. M. M. Motsa, T. A. M. Msagati, J. M. Thwala and B. B. Mamba, *Desalination and Water Treatment*, 2015, **53**, 2604-2612.
26. N. Keshavarzi, F. Mashayekhy Rad, A. Mace, F. Ansari, F. Akhtar, U. Nilsson, L. Berglund and L. Bergström, *ACS applied materials & interfaces*, 2015, **7**, 14254-14262.
27. R. Liu, W. Ji, W. Wang, Y. Li, L. Yin, Y. Song and G. He, *Separation and Purification Technology*, 2025, **361**, 131349.
28. M. K. Uddin, N. N. Abd Malek, A. H. Jawad and S. Sabar, *International Journal of Phytoremediation*, 2023, **25**, 393-402.
29. E. B. Khalifa, C. Cecone, B. Rzig, S. Azaiez, F. Cesano, M. Malandrino, P. Bracco and G. Magnacca, *Reactive and Functional Polymers*, 2023, **193**, 105763.
30. H. Kandil and H. Ali, *Journal of Polymers and the Environment*, 2023, **31**, 1456-1477.
31. A. M. Amin, H. A. Ibrahium, A. A. Gouda, R. E. Sheikh, B. M. Atia, M. A. Gado and N. S. Awwad, *International Journal of Environmental Analytical Chemistry*, 2024, 1-28.
32. S. Mahmoud, B. Atia and M. Gado, *International Journal of Environmental Science and Technology*, 2025, 1-26.
33. S. A. Mahmoud, B. M. Atia and M. Abdalla, *ChemistrySelect*, 2024, **9**, e202401169.
34. H. Isawi, *Arabian Journal of Chemistry*, 2020, **13**, 5691-5716.
35. J. H. Chen, G. P. Li, Q. L. Liu, J. C. Ni, W. B. Wu and J. M. Lin, *Chemical Engineering Journal*, 2010, **165**, 465-473.
36. X. Yang, T. Zhou, B. Ren, A. Hursthouse and Y. Zhang, *Scientific reports*, 2018, **8**, 10717.
37. Y. Li, J. Wen, Z. Xue, X. Yin, L. Yuan and C. Yang, *Journal of Hazardous Materials*, 2022, **426**, 127809.
38. Y. Nthwane, B. Fouda-Mbanga, M. Thwala and K. Pillay, *Environmental Technology*, 2025, **46**, 414-430.
39. C. Wang, J. Yu, K. Feng, L. Wang and J. Huang, *Microporous and Mesoporous Materials*, 2022, **345**, 112256.
40. D. N. Tran, A. M. Marti and K. J. Balkus Jr, *Fibers*, 2014, **2**, 308-318.
41. W. Zhan, C. Xu, G. Qian, G. Huang, X. Tang and B. Lin, *RSC advances*, 2018, **8**, 18723-18733.
42. J. Di, Z. Ruan, S. Zhang, Y. Dong, S. Fu, H. Li and G. Jiang, *Scientific Reports*, 2022, **12**, 1394.
43. A. N. Mohammed, *Environmental Monitoring and Assessment*, 2024, **196**, 611.
44. E. Hidayat, T. Yoshino, S. Yonemura, Y. Mitoma and H. Harada, *Materials*, 2023, **16**, 2532.
45. K. S. Sopanrao, A. Venugopal, C. M. Patel and I. Sreedhar, *Environmental Science and Pollution Research*, 2024, 1-22.
46. Y. Li, M. Tan, G. Liu, D. Si, N. Chen and D. Zhou, *Journal of Materials Chemistry A*, 2022, **10**, 6724-6730.
47. K. Wang, F. Zhang, K. Xu, Y. Che, M. Qi and C. Song, *RSC advances*, 2023, **13**, 6713-6736.
48. M. Yıldız Yiğit, E. S. Baran and Ç. K. Moral, *Water Science and Technology*, 2021, **83**, 1152-1166.
49. S. Shankari, S. Rajashalini, P. Gowri, R. Prabakaran and G. Punithakumari.
50. A. Gherasim, A. Dao and J. A. Bernstein, *World Allergy Organization Journal*, 2018, **11**, 29.

View Article Online
DOI: 10.1039/D5NA00996K

Data Availability Statement: The data supporting the findings of this study can be obtained from the corresponding author upon request. Due to privacy concerns and other restrictions, the data are not publicly accessible.